


Density effects on electronic configurations in dense plasmas

Gérald Faussurier* and Christophe Blancard

Commissariat à l'Énergie Atomique, DAM, DIF, F-91297 Arpajon, France

 (Received 24 October 2017; revised manuscript received 12 February 2018; published 28 February 2018)

We present a quantum mechanical model to describe the density effects on electronic configurations inside a plasma environment. Two different approaches are given by starting from a quantum average-atom model. Illustrations are shown for an aluminum plasma in local thermodynamic equilibrium at solid density and at a temperature of 100 eV and in the thermodynamic conditions of a recent experiment designed to characterize the effects of the ionization potential depression treatment. Our approach compares well with experiment and is consistent in that case with the approach of Stewart and Pyatt to describe the ionization potential depression rather than with the method of Ecker and Kröll.

DOI: [10.1103/PhysRevE.97.023206](https://doi.org/10.1103/PhysRevE.97.023206)

I. INTRODUCTION

Recently, experiments [1,2] were done to measure the ionization potential depression (IPD) in dense plasmas. The results were controversial since neither the method of Ecker and Kröll [3] nor the approach of Stewart and Pyatt [4] can reproduce the two experimental data sets. These experiments appeal for a better understanding of the IPD phenomenon [5,6] that plays a key role in equation of state or opacity calculations.

Due to IPD, the threshold energy to ionize a given ion by exciting one of the bound electrons to the continuum is lowered compared to the equivalent isolated ion. The bound state may or may not exist, impacting the ionization balance and the charge state distribution towards increasing ionization. The IPD is difficult to describe since this phenomenon is basically connected to the electrostatic potential distribution around an atomic species due to free electrons and neighboring ions. In this paper, we propose to describe the screening due to free electrons on a given electronic configuration immersed in a plasma, neglecting the influence of the neighboring ions on this electronic configuration. The background ionic system is described by a jellium that neutralizes the free electron distribution.

The present paper is organized as follows. In the first part, we present our approach to study the polarization around an electronic configuration in a plasma environment in local thermodynamic equilibrium (LTE) conditions. The basic tool is the average-atom model in a muffin-tin approximation [7–12]. First, we solve the nonrelativistic average-atom equations at given mass density ρ and electron temperature T . This gives us the chemical potential μ . For each electronic configuration, we then solve the average-atom equations under constraint given by the occupation probabilities of the subshells of a given electronic configuration in the nonrelativistic approximation. The bound and free electron wave functions are calculated at fixed chemical potential μ given by the average-atom model, the neutrality radius R_n being tuned in order to have Z electrons

in the neutrality cell. Z is the nuclear charge. The neutrality cell generalizes the notion of the Wigner-Seitz cell. We propose two approaches based on density functional theory (DFT) or *ad hoc* potentials from Hartree-Fock calculations [13] (HF). We allow the free electron density to polarize around the nucleus for each electronic configuration. Consequently, we have one particular neutrality radius R_n for each electronic configuration. We thus go beyond the simple approximation of constant free electron density inside the neutrality cell [14–17] as done also by Massacrier and coworkers [18–20]. In the present approach, we obtain naturally the shift in energy due to the electrostatic potential of the free electrons inside the neutrality cell, the effect of which should be added to the average configuration energy as a correction energy [21]. In the second part of the paper, we present applications of our approach to an aluminum plasma in LTE at solid density and at $T = 100$ eV. We also consider aluminum plasmas in thermodynamical conditions corresponding to the Hoarty *et al.* experiment [2]. In the last part of the paper, we present concluding remarks.

II. METHOD

The present method is a multistep approach. First, we perform calculations in the nonrelativistic approximation using an LTE average-atom model in a muffin-tin approximation [7–12] for a given element at constant mass density ρ and electron temperature T . We assume that the ion and electron temperatures are equal. The chemical potential μ is such that

$$\int_0^{R_{WS}} 4\pi r^2 [n_b(r) + n_f(r)] dr = Z, \quad (1)$$

where $n_b(r)$ and $n_f(r)$ are the bound and free electron densities of the average atom. R_{WS} is the Wigner-Seitz radius with $4\pi R_{WS}^3 N_i / 3 = 1$ where N_i is the ion density. The average-atom equations read

$$\left[-\frac{\hbar^2}{2m_e} \nabla^2 - \frac{Z^2 e^2}{r} + e^2 \int d\mathbf{r}' \frac{n(r')}{|\mathbf{r} - \mathbf{r}'|} + V_{xc}(r) \right] \psi_a(\mathbf{r}) = \varepsilon_a \psi_a(\mathbf{r}) \quad (2)$$

*Corresponding author: gerald.faussurier@cea.fr

where \hbar is the reduced Planck constant, e is the elementary charge, and m_e is the electron mass. ε_a is the one-electron energy. $a = (n, \ell)$ for bound states and $a = (\varepsilon, \ell)$ for continuum states. In this case, the one-electron energy is simply ε . $V_{xc}(r)$ is the exchange-correlation potential [22]. The wave function $\psi_a(\mathbf{r})$ is decomposed in a spherical basis:

$$\psi_a(\mathbf{r}) = \frac{1}{r} P_a(r) Y_{\ell_a}^{m_a}(\theta, \phi) \chi_{\sigma_a} \quad (3)$$

where $Y_{\ell}^m(\theta, \phi)$ is a spherical harmonic and χ_{σ} is a two-component electron spinor. The bound and free radial wave functions are normalized as

$$\int_0^{+\infty} dr P_{n\ell}(r) P_{n'\ell}(r) = \delta_{nn'} \quad (4)$$

and

$$\int_0^{+\infty} dr P_{\varepsilon\ell}(r) P_{\varepsilon'\ell}(r) = \delta(\varepsilon - \varepsilon'). \quad (5)$$

The total electron density of the average atom $n(r) = n_b(r) + n_f(r)$ where

$$4\pi r^2 n_b(r) = \sum_{n\ell} \frac{2(2\ell + 1)}{1 + e^{(\varepsilon_{n\ell} - \mu)/k_B T}} P_{n\ell}(r)^2 \quad (6)$$

and

$$4\pi r^2 n_f(r) = \sum_{\ell} \int_0^{+\infty} d\varepsilon \frac{2(2\ell + 1)}{1 + e^{(\varepsilon - \mu)/k_B T}} P_{\varepsilon\ell}(r)^2. \quad (7)$$

k_B is the Boltzmann constant.

Solving the average-atom equations is the first step. To go beyond, we need to describe an electronic configuration of interest including plasma effects. To achieve this task, one can adapt the simple average-atom model in the muffin-tin approximation. In short, we solve the average-atom equation at fixed occupation probabilities $f_{n\ell} = q_{n\ell}/D_{n\ell}$, i.e., the ones obtained from the subshell occupation numbers ($q_{n\ell}$) of the configuration. $D_{n\ell} = 2(2\ell + 1)$ is the degeneracy of subshell $n\ell$. The key problem concerns the electroneutrality condition [14]. One can no longer use the Wigner-Seitz radius and the chemical potential can no longer be adjusted because each configuration must see the same electron density at large radius. Keeping the chemical potential μ fixed, we propose to find the neutrality radius R_n for which

$$\int_0^{R_n} 4\pi r^2 n(r) dr = Z \quad (8)$$

where $n(r)$ is the sum of the bound and free electron densities associated to the particular electronic configuration inside the neutrality cell. We solve average-atom equations under constraint with an electroneutrality radius R_n to be determined during the self-consistent process of resolution of these effective average-atom equations. There is an electroneutrality radius for each electronic configuration. We expect R_n to be smaller (larger) than R_{WS} for an electronic configuration with a number of bound electrons larger (smaller) than the number of bound electrons of the average-atom model. This is the proposed DFT.

Another approach consists in using model or *ad hoc* potentials. To do so, we use either the Thomas-Fermi-Dirac-Amaldi

potential $V_{TF}(r)$ [13] or the optimized potential method (OPM) [23] and a plasma potential $V_p(r)$ [14]. Instead of Eq. (2), we solve

$$\left[-\frac{\hbar^2}{2m_e} \nabla^2 + V_{TF}(r) + V_p(r) \right] \psi_a(\mathbf{r}) = \varepsilon_a \psi_a(\mathbf{r}). \quad (9)$$

There is a subtlety between Eqs. (2) and (9). In Eq. (2), the plasma potential associated with $n_f(r)$ inside $[0, R_n]$ and determined by solving the related Poisson equation behaves as $(Z - N)e^2/r$ when $r \rightarrow +\infty$ whereas $V_{TF}(r) \sim -(Z - N + 1)e^2/r$ and $V_p(r) \sim (Z - N + 1)e^2/r$ when $r \rightarrow +\infty$. $N = \sum_{n\ell} q_{n\ell}$ is the number of bound electrons of the electronic configuration. $V_{TF}(r)$ represents the average effect of the $N - 1$ other bound electrons and of the nuclear charge for a given electron and $V_p(r)$ is the plasma potential. A similar trend is found for $V_{OPM}(r)$, which replaces $V_{TF}(r)$ in Eq. (9), in the OPM approach. First, we define a radius R_0 such that

$$\int_0^{R_0} 4\pi r^2 n_f(r) dr = Z - N + 1. \quad (10)$$

Then, we can use the potential proposed by Massacrier and Dubau [14], i.e.,

$$V_p(r) = \frac{(Z - N + 1)e^2}{2R_0} \left[3 - \left(\frac{r}{R_0} \right)^2 \right] \quad (11)$$

if $r < R_0$ and

$$V_p(r) = \frac{(Z - N + 1)e^2}{r} \quad (12)$$

if $r > R_0$. This is the proposed HF. For OPM, R_0 is such that $4\pi R_0^3 N_e/3 = Z - N + 1$ where N_e is the electron density. Note that in OPM one does not consider free electrons when solving Eq. (9) with $V_{OPM}(r)$ instead of $V_{TF}(r)$. Moreover, one treats the potential $V_p(r)$ by perturbation.

Once one has solved the effective average-atom equations, one can calculate the configuration average energy of the given configuration [21] as well as the contribution of the free electron electrostatic potential [14,15] to this energy. This kind of approach does not rely on the *ad hoc* continuum lowering model [3,4] since plasma effects are taken into account in a self-consistent way once one knows the free electron electrostatic potential, the bound electron wave functions, and the occupation numbers of the electronic configuration [14,15]. The self-consistency is obtained between the bound and free one-electron wave functions and the neutrality radius. The configuration average energy of a given configuration reads [21]

$$E_{av} = E_{conf} + \Delta E_r + \Delta E_p \quad (13)$$

where

$$E_{conf} = \sum_a \left\{ q(a) I(a) + \frac{1}{2} q(a) [q(a) - 1] A v(a, a) \right\} + \frac{1}{2} \sum_{a \neq b} [q(a) q(b) A v(a, b)], \quad (14)$$

$$I(a) = \varepsilon_a - \int_0^{+\infty} dr P_a(r)^2 \left[V(r) + \frac{Z e^2}{r} \right], \quad (15)$$

$$Av(a,a) = F^0(a,a) - \frac{2\ell_a + 1}{4\ell_a + 1} \sum_{k>0} \begin{pmatrix} \ell_a & \ell_a & k \\ 0 & 0 & 0 \end{pmatrix}^2 F^k(a,a), \quad (16)$$

$$Av(a,b) = F^0(a,b) - \frac{1}{2} \sum_k \begin{pmatrix} \ell_a & \ell_b & k \\ 0 & 0 & 0 \end{pmatrix}^2 G^k(a,b), \quad (17)$$

and

$$\Delta E_p = \sum_a \int_0^{+\infty} dr V_p(r) P_a(r)^2. \quad (18)$$

In DFT, $V(r) = -\frac{Z^2 e^2}{r} + e^2 \int d\mathbf{r}' \frac{n(r')}{|\mathbf{r}-\mathbf{r}'|} + V_{xc}(r)$ whereas $V(r) = V_{TF}(r) + V_p(r)$ in HF. $F^k(a,b) = e^2 R^k(a,b,a,b)$ and $G^k(a,b) = e^2 R^k(a,b,b,a)$ where

$$R^k(a,b,c,d) = \int_0^{+\infty} dr_1 \int_0^{+\infty} dr_2 P_a(r_1) P_b(r_2) P_c(r_1) \times P_d(r_2) \frac{r_{<}^k}{r_{>}^{k+1}}. \quad (19)$$

$r_{<} = \min(r_1, r_2)$ and $r_{>} = \max(r_1, r_2)$. Moreover, ΔE_r is a relativistic correction following Cowan [24].

When $Av(a,a)$ and $Av(a,b)$ are calculated using the average-atom data, we can estimate the ionization variance using the classical theory of fluctuations [25–27]. We consider the matrix

$$\omega_{i,j} = \frac{\delta_{i,j}}{D_i f_i g_i} + Av(i,j)/k_B T \quad (20)$$

where D_i is the degeneracy of subshell i . Here, f_i is defined as

$$f_i = \frac{1}{1 + e^{(\varepsilon_i - \mu)/k_B T}}, \quad (21)$$

and

$$g_i = 1 - f_i = \frac{1}{1 + e^{-(\varepsilon_i - \mu)/k_B T}}. \quad (22)$$

The ionization variance σ_Z^2 is given by

$$\sigma_Z^2 \approx \sum_{i,j} (\omega^{-1})_{i,j}. \quad (23)$$

Due to density effects, many interesting questions arise. The selected configuration may be shown to not exist if one of its bound shells goes into the continuum. Resonances can be encountered in the continuum during the resolution of the equations for each electronic configuration immersed in a plasma [15]. Due to screening, orbitals that are not bound in the average atom can be shown to be bound for some particular configuration. So electronic configurations eliminated from the knowledge of the average-atom configuration can indeed exist due to plasma effects. This means that the configuration sampling should be as efficient as possible. These questions are not trivial. They can impact the calculation of emissivity and opacity, for instance [1,2,5].

III. APPLICATIONS

We consider an aluminum plasma in LTE at solid density and $T = 100$ eV. We give in Table I E_{conf} , ΔE_r , and ΔE_p using the DFT, HF, and OPM approaches. The average-atom configuration is $1s^2 2s^{0.74} 2p^{1.83} 3s^{0.15} 3p^{0.42} 3d^{0.62}$ and so nearly $1s^2 2s^2 p^2$, which is the most probable electronic configuration. Concerning the relativistic correction, OPM and DFT agree with each other. There are two groups. The relativistic correction ΔE_r is small and close to the reference energy of the average-atom model, which is -0.4355 hartree. This reference energy comes from the treatment of the exchange-correlation phenomena. As for the three approaches, the Hartree-Fock energies E_{conf} are relatively close to each other, the difference being the plasma correction ΔE_p . There is a noticeable fact to remark. We can see that ΔE_p increases from configuration $1s^2$ up to configuration $1s^2 2s^2 2p^4$ for OPM and HF and then decreases up to configuration $1s^2 2s^2 2p^6$. The change in behavior occurs around configuration $1s^2 2s^2 2p^3$ for DFT. This fact is the manifestation of the competition between $V_p(r)$ and the configuration population. When one adds an electron, the potential $V_p(r)$ decreases through the factor $Z - N + 1$ for OPM and HF, and $Z - N$ for DFT, but the number of electron increases by one unit. From Eq. (18), one can see the competition. Here, the decrease of $V_p(r)$ is not balanced

TABLE I. Atomic data using DFT, HF, and OPM approaches in an aluminum plasma in LTE at solid density and $T = 100$ eV (the hartree energy unit is used).

Configuration	DFT			HF			OPM		
	E_{conf}	ΔE_r	ΔE_p	E_{conf}	ΔE_r	ΔE_p	E_{conf}	ΔE_r	ΔE_p
$1s^2$	-160.9826	-0.3490	11.0863	-160.9858	-0.3506	10.5798	-160.9861	-0.3515	10.1066
$1s^2 2s$	-177.1798	-0.3890	15.1227	-177.1711	-0.3816	14.8782	-177.1860	-0.3928	14.2670
$1s^2 2s^2$	-191.6368	-0.4245	18.3218	-191.5878	-0.4074	18.3490	-191.6432	-0.4288	17.8182
$1s^2 2s^2 2p$	-203.7591	-0.4318	20.8196	-203.6367	-0.4081	21.0926	-203.7680	-0.4368	20.7362
$1s^2 2s^2 2p^2$	-214.1073	-0.4365	23.8432	-213.9139	-0.4092	23.6689	-214.1230	-0.4423	22.9708
$1s^2 2s^2 2p^3$	-222.7936	-0.4398	24.9291	-222.5686	-0.4109	25.0410	-222.8145	-0.4458	24.4723
$1s^2 2s^2 2p^4$	-229.9252	-0.4418	24.5706	-229.7285	-0.4134	25.8157	-229.9506	-0.4476	25.1770
$1s^2 2s^2 2p^5$	-235.6097	-0.4426	23.1004	-235.4950	-0.4168	25.5035	-235.6412	-0.4482	25.0001
$1s^2 2s^2 2p^6$	-239.9561	-0.4425	20.6221	-239.9244	-0.4210	24.1339	-239.9985	-0.4478	23.8225

TABLE II. R_n and R_0 predicted by the HF approach in an aluminum plasma in LTE at solid density and $T = 100$ eV. R_n and R_0 are in units of Bohr radius a_0 .

Configuration	R_n	R_0
$1s^2$	3.2831	3.4009
$1s^2 2s$	3.1928	3.3154
$1s^2 2s^2$	3.1237	3.2515
$1s^2 2s^2 2p$	3.0428	3.1774
$1s^2 2s^2 2p^2$	2.8625	3.0139
$1s^2 2s^2 2p^3$	2.7361	2.9019
$1s^2 2s^2 2p^4$	2.5651	2.7498
$1s^2 2s^2 2p^5$	2.3938	2.6012
$1s^2 2s^2 2p^6$	2.1932	2.4338

by the increase of the configuration population. This is a subtle dense plasma effect predicted by the two models. One cannot then speak always of continuum lowering. It is not clear if it is a physical effect or a limitation of the models. For completeness, we give in Table II R_n and R_0 predicted by HF. As for the average-atom model, $R_n = 2.9905 a_0$ where a_0 is the Bohr radius. Note that the convergence of the scheme involving a fixed electronic configuration in a dense plasma can be difficult due to the presence of resonances in the continuum [18–20]. These resonances can be very sharp and so not easy to carefully describe.

What should be seen is the existence of electronic configurations forbidden by the average-atom model. In the case we consider, in the average atom only orbitals $1s$ to $3d$ exist. However, orbitals with principal quantum number 4 may exist in some particular electronic configurations. To find them, one should adjust screening. The idea is to reduce screening in order to bound an orbital with principal quantum number 4. This is obtained by depopulating inner orbitals. The two approaches agree to predict the nonexistence of configurations $1s^2 4p$, $1s^2 4d$, and $1s^2 4f$. Concerning $1s 4s$, all the approaches predict its existence whereas $1s 4p$ is predicted to exist only by HF. Again, DFT and HF predict the nonexistence of $1s 4d$ and $1s 4f$ due to density effects. We summarize in Table III our search.

In the case we consider, the aluminum plasma ionization balance has been also calculated. Figure 1 shows the results. For the ionic state between 4 and 11, the excited configuration

TABLE III. Configuration existence as a function of DFT and HF approaches in an aluminum plasma in LTE at solid density and $T = 100$ eV.

Configuration	DFT	HF
$1s^2 4s$	∅	∅
$1s^2 4p$	∅	∅
$1s^2 4d$	∅	∅
$1s^2 4f$	∅	∅
$1s 4s$	∃	∃
$1s 4p$	∅	∃
$1s 4d$	∅	∅
$1s 4f$	∅	∅

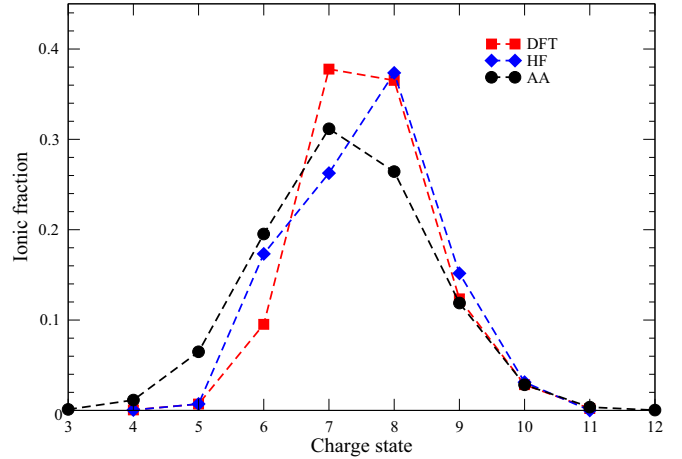


FIG. 1. Ionic fractions predicted by the average-atom model (AA), DFT, and HF approaches in an aluminum plasma in LTE at solid density and $T = 100$ eV.

sampling has been restricted to double excitations from any subshell of each ground configuration. In the present case, the orbitals we consider are up to $4f$ allowing us to generate 1337 nonrelativistic configurations. The average-atom chemical potential is used for the overall configuration energy calculations. $V_{\text{TF}}(r)$ is used as an *ad hoc* potential in the HF model. Due to density effects, only 345 and 343 configurations are retained by the DFT and HF models, respectively. For both DFT and HF models, excited configurations involving $4s$ and $4p$ orbitals are kept for the two-electron system. For the three-electron system, the DFT model keeps singly and doubly inner-shell excited configurations involving the $4s$ orbital. The HF model does not retain such highly excited configurations. For each configurations set, the Saha-Boltzmann equations have been solved using the average-atom chemical potential. The mean ionizations and the ionization variances, obtained using the configuration occupation probabilities, are reported in Table IV. They are compared to corresponding average-atom values where the ionization variance has been deduced from the classical theory of fluctuations. In the present case, the DFT and HF mean ionizations are a little bit larger than the average-atom value. The DFT and HF ionization variances are noticeably reduced compared to the average-atom value. The HF ionization skewness value is typically ten times lower than the DFT value because the C-like and the N-like systems do not involve the same configuration numbers for HF and DFT calculations. For the C(N)-like system, 56(51) and 77(43) configurations are retained for HF and DFT calculations, respectively. For these two charge states, Fig. 2 shows the

TABLE IV. Average ionization and ionization variance for the average atom model (AA), DFT, and HF approaches in an aluminum plasma in LTE at solid density and $T = 100$ eV.

Model	Average ionization	Ionization variance	Skewness
AA	7.2391	1.5788	0
DFT	7.5950	0.9241	-0.229923
HF	7.5819	1.1288	-0.0216070

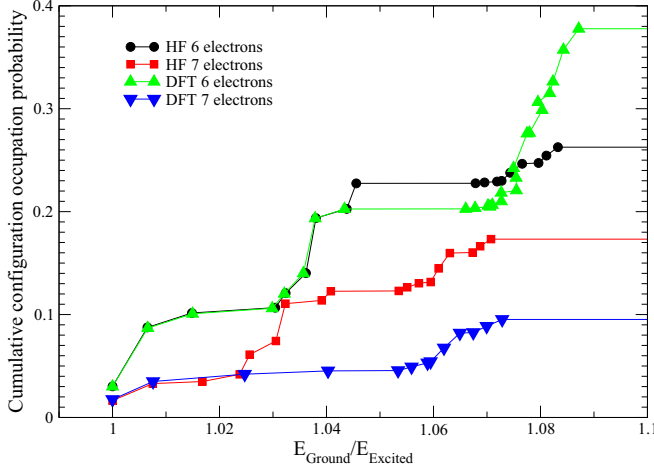


FIG. 2. DFT and HF cumulative configuration occupation probabilities as a function of the ratio of the ground configuration energy (E_{ground}) on the excited configuration energy (E_{excited}) in an aluminum plasma in LTE at solid density and $T = 100$ eV.

cumulative configuration occupation probabilities as a function of the ratio of the ground configuration energy (E_{ground}) on the excited configuration energy (E_{excited}). The effects of excited configurations are clearly visible for $E_{\text{ground}}/E_{\text{excited}}$ values around 1.03 and above 1.075 for N-like and C-like systems, respectively.

We also consider aluminum plasmas in thermodynamical conditions corresponding to the Hoarty *et al.* experiment [2]. Assuming LTE, ionization balances have been calculated using the HF model [and $V_{\text{TF}}(r)$ as *ad hoc* potential] for the following mass density and temperature conditions: 1.2 g/cc, 550 eV; 2.5 g/cc, 650 eV; 4 g/cc, 700 eV; 5.5 g/cc, 550 eV; and 9 g/cc, 700 eV. From the low to the high density cases, the mean ionization values resulting from the Saha-Boltzmann equilibrium are 12.3927(12.3574), 12.4743(12.4689), 12.3857(12.3749), 11.6922(11.6501), and 12.1187(12.0939) where average-atom

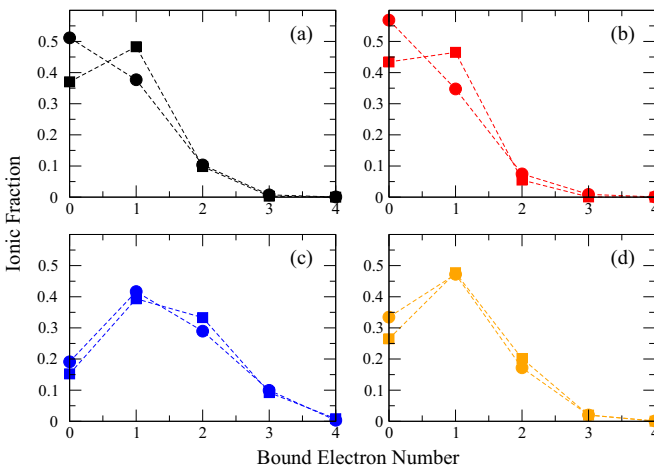


FIG. 3. Ionic fractions predicted by the average-atom model (AA, square symbol) and HF (circle symbol) approaches in an aluminum plasma in LTE for the following mass density and temperature conditions: (a) 1.2 g/cc, 550 eV; (b) 2.5 g/cc, 650 eV; (c) 5.5 g/cc, 550 eV; (d) 9 g/cc, 700 eV.

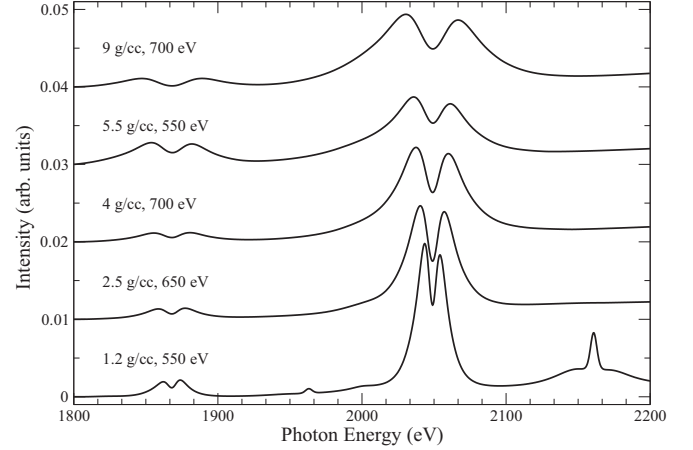


FIG. 4. Synthetic spectra for aluminum plasmas in LTE. From bottom to top, the thermodynamical conditions are 1.2 g/cc, 550 eV; 2.5 g/cc, 650 eV; 4 g/cc, 700 eV; 5.5 g/cc, 550 eV; and 9 g/cc, 700 eV.

values are given in parentheses. Figure 3 shows the ionic fraction distributions. HF results are compared to corresponding average-atom values where the ionization variance has been deduced from the classical theory of fluctuations. The 4-g/cc, 700-eV case has been omitted because the corresponding HF and average-atom model ionization balances are close to those of the 1.2-g/cc, 550-eV case. For the lowest density case, excited configurations involving orbitals with principal quantum number up to $n = 4$ are kept up to four-electron ions. For the higher densities such excited configurations do not exist. For the highest density case, excited configurations involving orbitals up to $3d$ are kept only for the H-like and He-like ions. These results confirm the predictions of simulations using the Steward-Pyatt model of IPD [2]. Based on the configuration occupation probabilities deduced from the Saha-Boltzmann equilibrium, synthetic spectra have been computed for each (ρ, T) case in the 1.8–2.2-keV photon energy range. The spectra have been convoluted with a Gaussian profile with a full width at half maximum equal to 4 eV to take into account the spectral resolution ($E/\delta E = 500$) [2]. Figure 4 shows the spectra. The curves are normalized to unity in the considered photon energy range and they have been shifted in intensity for clarity. In all cases Stark broadened Ly_{β} and He_{β} lines can be observed. The Stark broadened $n = 1-4$ line transitions are visible from the lowest density case only. Our results compare well with experiment [2].

IV. CONCLUSION

We have proposed a consistent method to describe the density effects on electronic configurations in dense plasmas. This method does not rely on *ad hoc* ionization potential lowering. Results show the difficulty to treat density effects on electronic structure. Statistical methods based on the average-atom model to select which electronic configuration exists or not may fail due to dense plasmas effects. Once a selected set of electronic configurations has been determined, the present approach is well suited to describe LTE but also non-LTE plasmas using high performance computing systems if the free electrons are in LTE.

- [1] O. Ciricosta, S. M. Vinko, H. K. Chung, B. I. Cho, C. R. D. Brown, T. Burian, J. Chalupsky, K. Engelhorn, R. W. Falcone, C. Graves, V. Hajkova, A. Higginbotham, L. Juha, J. Krzywinski, H. J. Lee, M. Messerschmidt, C. D. Murphy, Y. Ping, D. S. Rackstraw, A. Scherz, W. Schlotter, S. Toleikis, J. J. Turner, L. Vysin, T. Wang, B. Wu, U. Zastra, D. Zhu, R. W. Lee, P. Heimann, B. Nagler, and J. S. Wark, *Phys. Rev. Lett.* **109**, 065002 (2012).
- [2] D. J. Hoarty, P. Allan, S. F. James, C. R. D. Brown, L. M. R. Hobbs, M. P. Hill, J. W. O. Harris, J. Morton, M. G. Brookes, R. Shepherd, J. Dunn, H. Chen, E. Von Marley, P. Beiersdorfer, H. K. Chung, R. W. Lee, G. Brown, and J. Emig, *Phys. Rev. Lett.* **110**, 265003 (2013).
- [3] G. Ecker and W. Kröll, *Phys. Fluids* **6**, 62 (1963).
- [4] J. C. Stewart and K. D. Pyatt, *Astrophys. J.* **144**, 1203 (1966).
- [5] C. A. Iglesias, *High Energy Dens. Phys.* **12**, 5 (2014).
- [6] S. K. Son, R. Thiele, Z. Jurek, B. Ziaja, and R. Santra, *Phys. Rev. X* **4**, 031004 (2014).
- [7] R. P. Feynman, N. Metropolis, and E. Teller, *Phys. Rev.* **75**, 1561 (1949).
- [8] B. F. Rozsnyai, *Phys. Rev. A* **5**, 1137 (1972).
- [9] D. A. Liberman, *Phys. Rev. B* **20**, 4981 (1979).
- [10] B. Wilson, V. Sonnad, P. Sterne, and W. Isaacs, *J. Quant. Spectrosc. Radiat. Transf.* **99**, 658 (2006).
- [11] W. R. Johnson, C. Guet, and G. F. Bertsch, *J. Quant. Spectrosc. Radiat. Transf.* **99**, 327 (2006).
- [12] M. S. Murillo, J. Weisheit, S. B. Hansen, and M. W. C. Dharma-Wardana, *Phys. Rev. E* **87**, 063113 (2013).
- [13] W. Eissner and H. Nussbaumer, *J. Phys. B* **2**, 1028 (1969).
- [14] G. Massacrier and J. Dubau, *J. Phys. B* **23**, 2459S (1990).
- [15] T. Vallotton, O. Peyrusse, and D. Benredjem, *J. Phys. B* **43**, 155207 (2010).
- [16] M. Belkhiri and M. Poirier, *Phys. Rev. A* **90**, 062712 (2014).
- [17] M. Belkhiri, C. J. Fontes, and M. Poirier, *Phys. Rev. A* **92**, 032501 (2015).
- [18] G. Massacrier, *J. Quant. Spectrosc. Radiat. Transfer* **51**, 221 (1994).
- [19] A. Y. Potekhin, G. Massacrier, and G. Chabrier, *Phys. Rev. E* **72**, 046402 (2005).
- [20] G. Massacrier, A. Y. Potekhin, and G. Chabrier, *Phys. Rev. E* **84**, 056406 (2011).
- [21] E. U. Condon and H. Odabaşı, *Atomic Structure* (Cambridge University, Cambridge, England, 1980).
- [22] H. Iyetomi and S. Ichimaru, *Phys. Rev. A* **34**, 433 (1986).
- [23] J. D. Talman and W. F. Shadwick, *Phys. Rev. A* **14**, 36 (1976).
- [24] R. D. Cowan, *The Theory of Atomic Structure and Spectra* (Berkeley, University of California, Berkeley, 1981).
- [25] L. Landau and E. Lifchitz, *Physique Statistique* (Editions Mir, Moscow, 1984).
- [26] F. Perrot, *Physica A* **150**, 357 (1988).
- [27] G. Faussurier, C. Blancard, and A. Decoster, *Phys. Rev. E* **56**, 3474 (1997).